ISSN No: -2456-2165 https://doi.org/10.38124/ijisrt/26mar1483

Quantitative Electrical Resistivity–Based Assessment of Subsurface Corrosion Risk for Buried Pipelines and Underground Facilities in the Niger Delta, Southern Nigeria

Tamunosiki Dieokuma[1]; Collins Chiemeke[2]

[1]Department of Physics, Federal University Otuoke, Bayelsa State, Nigeria
[2]Department of Physics, Federal University Otuoke, Bayelsa State, Nigeria

Publication Date: 2026/04/04

Abstract: Electrical resistivity investigations were carried out to quantitatively evaluate subsurface corrosion risk associated with buried pipelines and underground facilities at a gas flow station in southern Nigeria. Vertical Electrical Sounding (VES) data were acquired using the Schlumberger electrode configuration to determine the spatial distribution of subsurface electrical resistivity. Apparent resistivity values measured in the field were inverted to obtain true resistivity models, which were subsequently integrated into one-dimensional (1D), two-dimensional (2D), and three-dimensional (3D) resistivity representations, as well as depth-slice contour maps.

The results reveal a laterally continuous near-surface layer with resistivity values predominantly exceeding 1700Ωm to a depth of approximately 5m. Based on established corrosion-risk classification criteria, materials with resistivity values greater than 200Ωm are considered to pose low corrosion risk to buried metallic infrastructure. In contrast, resistivity values below 100Ωm, identified at greater depths, correspond to clay-rich horizons associated with elevated corrosion potential. These findings indicate that pipelines installed within the upper 5m are unlikely to experience corrosion driven by galvanic or stray electrical currents. However, isolated low-resistivity anomalies were detected and require localized remediation through soil replacement or enhanced corrosion-control measures. The study demonstrates the effectiveness of electrical resistivity surveying as a non-intrusive and quantitative tool for pre-construction corrosion-risk assessment in pipeline engineering.

Keywords: *Electrical Resistivity; Corrosion Risk; Buried Pipelines; Schlumberger Array; Engineering Geophysics; Niger Delta.*

How to Cite: Tamunosiki Dieokuma; Collins Chiemeke (2026) Quantitative Electrical Resistivity–Based Assessment of Subsurface Corrosion Risk for Buried Pipelines and Underground Facilities in the Niger Delta, Southern Nigeria. *International Journal of Innovative Science and Research Technology*, 11(3), 3146-3158. https://doi.org/10.38124/ijisrt/26mar1483

I. INTRODUCTION

Corrosion remains one of the principal threats to the integrity and service life of buried metallic pipelines and underground facilities. The susceptibility of such infrastructure to corrosion is strongly influenced by the electrical properties of surrounding soils, particularly electrical resistivity. Low-resistivity soils facilitate the movement of ionic currents and enhance electrochemical reactions that accelerate metal deterioration, whereas high-resistivity materials inhibit current flow and reduce corrosion rates.

Electrical resistivity methods provide a cost-effective and non-destructive means of characterising subsurface electrical properties and have been widely applied in hydrogeological, environmental, and geotechnical investigations. In recent years, their application has expanded to include corrosion-risk assessment for buried pipelines, where resistivity serves as a proxy indicator for soil aggressiveness.

Despite the widespread use of resistivity surveys, many site investigations rely on qualitative interpretations that limit their engineering relevance. This study addresses this limitation by applying a quantitatively constrained electrical resistivity approach to evaluate subsurface corrosion risk at a gas flow station. The objective is to delineate resistivity-controlled lithological units and establish safe burial depths for pipelines and underground facilities based on well-defined corrosion-risk thresholds.

ISSN No: -2456-2165 https://doi.org/10.38124/ijisrt/26mar1483

➢ *Geological and Environmental Setting*

The study area is located within the sedimentary framework of the Niger Delta Basin, which comprises thick sequences of unconsolidated to poorly consolidated sands and clays deposited under fluvial, deltaic, and shallow marine conditions. Near-surface sediments are dominated by continental sands of the Benin Formation, interbedded locally with clay lenses derived from the Ogwashi–Asaba Formation.

These sediments exhibit strong lateral and vertical heterogeneity in grain size, clay content, and moisture retention, resulting in pronounced spatial variations in electrical resistivity. Sandy units generally display high resistivity due to low clay content and reduced ionic conduction, whereas clay-rich horizons retain moisture and dissolved ions, producing low resistivity and increased corrosion potential. Understanding this resistivity variability is therefore essential for reliable engineering design and corrosion control.

II. MATERIALS AND METHODS

➢ *Data Acquisition*

Electrical resistivity measurements were acquired using the Schlumberger Vertical Electrical Sounding technique. Four electrodes were inserted into the ground along predefined survey points, consisting of two outer current electrodes and two inner potential electrodes. During acquisition, the spacing between current electrodes was progressively increased to probe deeper subsurface layers, while the potential electrode spacing was kept relatively constant and expanded only when necessary to maintain measurable potential differences. Subsurface resistance values were measured using a digital terrameter and recorded systematically for each electrode configuration until the maximum spread length was achieved.

➢ *Data Processing and Modelling*

Measured resistance values were converted to apparent resistivity using the appropriate geometric factors. The apparent resistivity data were then inverted using iterative inversion algorithms to obtain true subsurface resistivity models. Individual VES interpretations yielded 1D layered resistivity models, which were spatially correlated to generate 2D resistivity sections.

All VES datasets were further integrated to produce a 3D resistivity model of the study area. To enhance engineering interpretation, resistivity values at selected depths (0m, 5m, 30m, and 45m) were extracted to generate contour maps illustrating lateral resistivity variations at depths relevant to pipeline installation.

III. RESULTS

The resistivity models reveal a consistent subsurface structure across the study area. Near-surface resistivity values range from approximately 500Ωm to over 1700Ωm and extend to an average depth of 5m. This high-resistivity layer is interpreted as predominantly sandy material with low moisture content.

Beneath this layer, resistivity values decrease sharply to typical values between 50Ωm and 120Ωm at depths of approximately 20–30m, indicating clay-rich horizons with higher electrical conductivity. At greater depths, resistivity responses vary laterally, reflecting interbedded sand and clay units characteristic of deltaic depositional environments.

Depth-slice contour maps confirm that high-resistivity materials dominate the shallow subsurface, while low-resistivity anomalies are localized and discontinuous.

Table 1 Current Electrode Spacing, Potential Electrode Spacing, Measured Resistance, and Calculated Apparent Resistivity(Ωm) for VES1

AB/2 (m)	Resistance (Ω)	Mn/2 (m)	Apparent Resistivity(Ωm)
1	319.81	0.5	1005.117143
1.5	144.98	0.5	1025.215714
2	68.488	0.5	860.992
3	29.613	0.5	837.6248571
5	7.9406	0.5	623.9042857
7	2.8077	0.5	432.3858
7	26.159	3	671.4143333
10	6.4295	3	336.7833333
15	1.7515	3	206.4267857
20	0.65318	3	136.8567619
25	0.3628	3	118.7738095
30	0.26506	3	124.9568571
35	0.12378	3	79.4255
40	0.19651	3	164.6940952
45	0.11056	3	117.2725714
50	0.13325	3	174.4940476
55	0.20228	3	320.5174762

ISSN No: -2456-2165 https://doi.org/10.38124/ijisrt/26mar1483

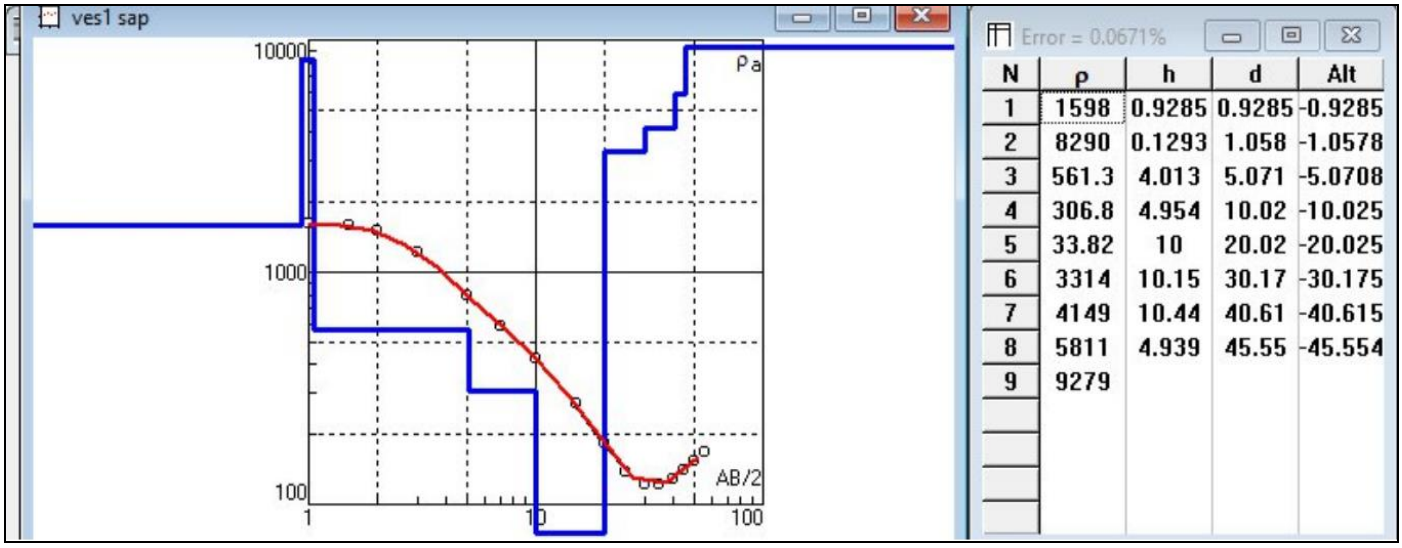

Fig 1 1D Electrical Resistivity Model for VES1

Table 2 Current Electrode Spacing, Potential Electrode Spacing, Measured Resistance, and Calculated Apparent Resistivity(Ωm) for VES2

AB/2 (m)	Resistance (Ω)	Mn/2 (m)	Apparent Resistivity(Ωm)
1	203.31	0.5	638.9742857
1.5	49.443	0.5	349.6326429
2	28.236	0.5	354.9668571
3	14.927	0.5	422.2208571
5	5.3523	0.5	420.5378571
7	2.1412	0.5	329.7448
7	25.307	3	649.5463333
10	6.9388	3	363.4609524
15	1.6381	3	193.0617857
20	0.63228	3	132.4777143
25	0.36772	3	120.3845238
30	0.24519	3	115.5895714
35	0.21779	3	139.7485833
40	0.26192	3	219.5139048
45	0.19692	3	208.8758571
50	0.17256	3	225.9714286
55	0.075603	3	119.7947536

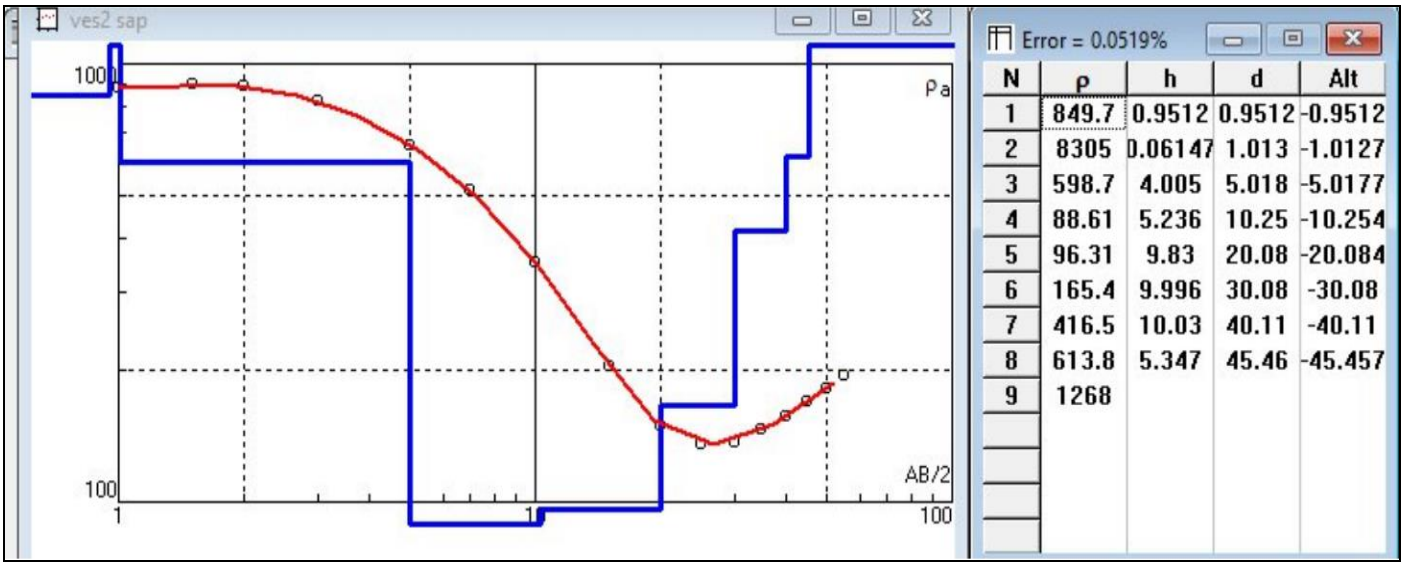

Fig 2 1D Electrical Resistivity Model for VES2

ISSN No: -2456-2165 https://doi.org/10.38124/ijisrt/26mar1483

Table 3 Current Electrode Spacing, Potential Electrode Spacing, Measured Resistance, and Calculated Apparent Resistivity(Ωm) for VES3

AB/2 (m)	Resistance (Ω)	Mn/2 (m)	Apparent Resistivity(Ωm)
1	181.53	0.5	570.5228571
1.5	54.379	0.5	384.5372143
2	15.791	0.5	198.5154286
3	5.5237	0.5	156.2418
5	1.2987	0.5	102.0407143
7	0.52804	0.5	81.31816
7	4.6908	3	120.3972
10	1.6141	3	84.54809524
15	0.77341	3	91.15189286
20	0.43365	3	90.86
25	0.27506	3	90.04940476
30	0.22318	3	105.2134286
35	0.15758	3	101.1138333
40	0.11955	3	100.1942857
45	0.34603	3	367.0389643
50	0.14672	3	192.1333333
55	0.06643	3	105.2599167

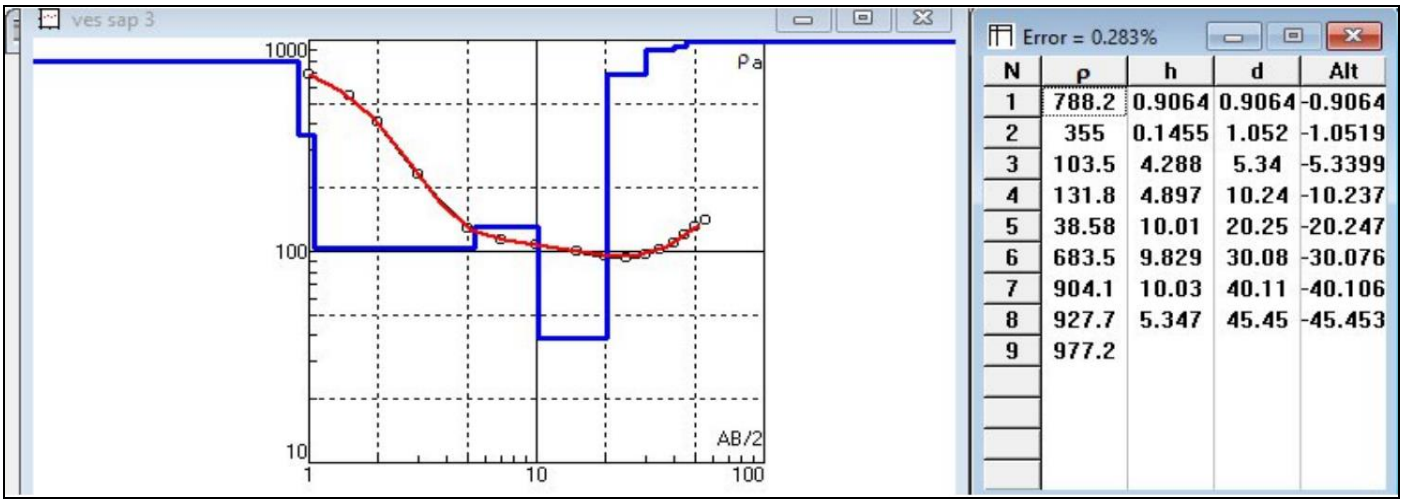

Fig 3 1D Electrical Resistivity Model for VES3

Table 4 Current Electrode Spacing, Potential Electrode Spacing, Measured Resistance, and Calculated Apparent Resistivity(Ωm) for VES4

AB/2 (m)	Resistance (Ω)	Mn/2 (m)	Apparent Resistivity(Ωm)
1	172.33	0.5	541.6085714
1.5	64.904	0.5	458.964
2	22.05	0.5	277.2
3	5.9955	0.5	169.587
5	1.0919	0.5	85.79214286
7	0.40562	0.5	62.46548
7	5.4486	3	139.8474
10	2.7602	3	144.5819048
15	1.464	3	172.5428571
20	1.0006	3	209.6495238
25	0.49009	3	160.446131
30	0.25721	3	121.2561429
35	0.12663	3	81.25425
40	0.10071	3	84.40457143
45	0.12542	3	133.0347857
50	0.024479	3	32.05583333
55	0.049084	3	77.77476667

ISSN No: -2456-2165 https://doi.org/10.38124/ijisrt/26mar1483

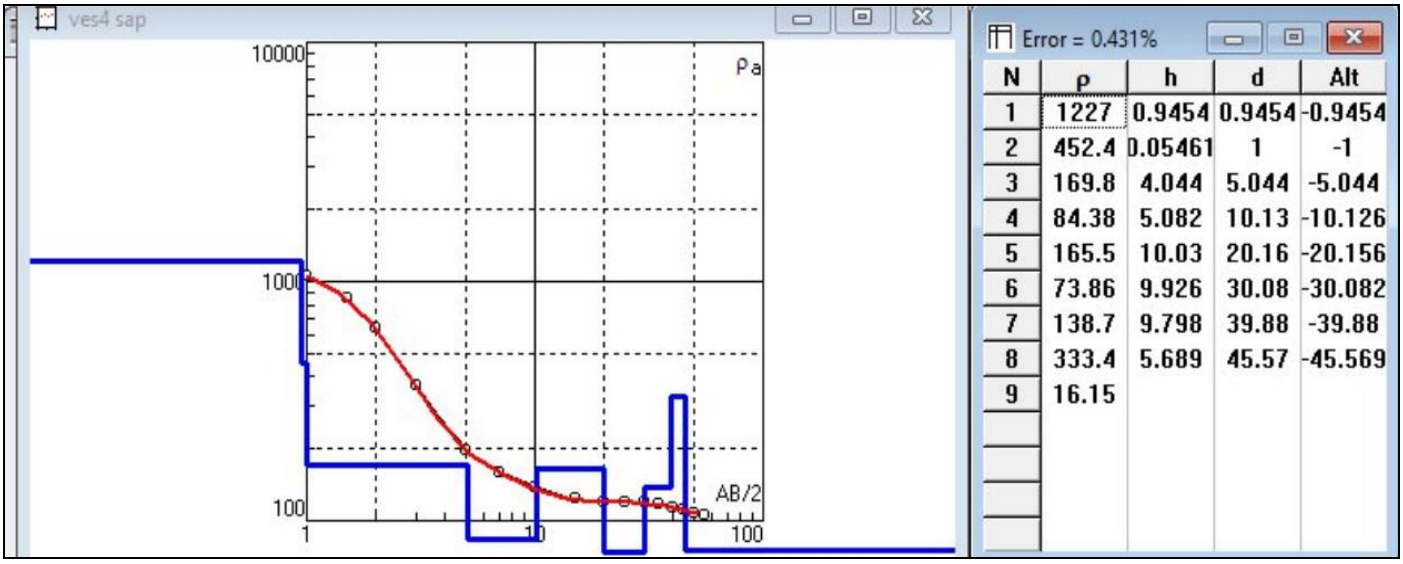

Fig 4 1D Electrical Resistivity Model for VES4

Table 5 Current Electrode Spacing, Potential Electrode Spacing, Measured Resistance, and Calculated Apparent Resistivity(Ωm) for VES5

AB/2 (m)	Resistance (Ω)	Mn/2 (m)	Apparent Resistivity(Ωm)
1	111.21	0.5	349.5171429
1.5	53.618	0.5	379.1558571
2	21.287	0.5	267.608
3	11.029	0.5	311.9631429
5	2.0841	0.5	163.7507143
7	0.78703	0.5	121.20262
7	6.2776	3	161.1250667
10	2.0422	3	106.972381
15	1.0415	3	122.7482143
20	0.60301	3	126.3449524
25	0.50263	3	164.5514881
30	0.27355	3	128.9592857
35	0.15589	3	100.0294167
40	0.64771	3	542.8426667
45	0.43624	3	462.726
50	0.15053	3	197.122619
55	0.1163	3	184.280119

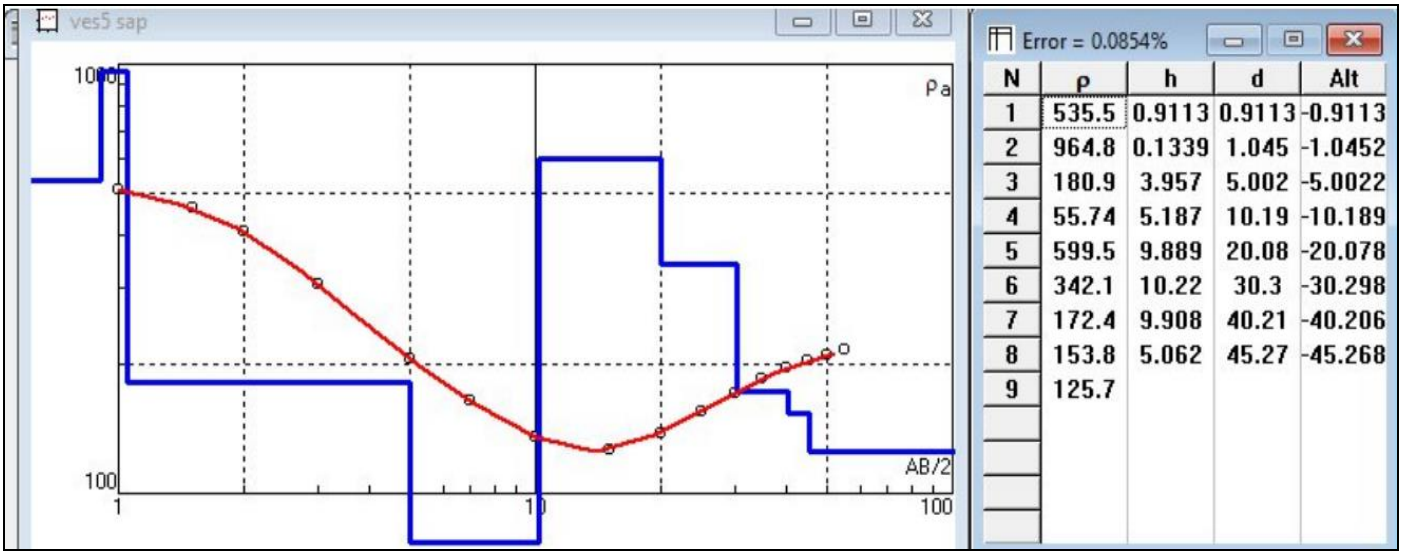

Fig 5 1D Electrical Resistivity Model for VES5

ISSN No: -2456-2165 https://doi.org/10.38124/ijisrt/26mar1483

Table 6 Current Electrode Spacing, Potential Electrode Spacing, Measured Resistance, and Calculated Apparent Resistivity(Ωm) for VES6

AB/2 (m)	Resistance (Ω)	Mn/2 (m)	Apparent Resistivity(Ωm)
1	138.2	0.5	434.3428571
1.5	49.796	0.5	352.1288571
2	19.157	0.5	240.8308571
3	5.009	0.5	141.6831429
5	0.95683	0.5	75.1795
7	0.4953	0.5	76.2762
7	5.4432	3	139.7088
10	2.552	3	133.6761905
15	1.2741	3	150.1617857
20	0.7757	3	162.527619
25	0.48341	3	158.2592262
30	0.3174	3	149.6314286
35	0.20548	3	131.8496667
40	0.17654	3	147.9573333
45	0.13839	3	146.79225
50	0.083561	3	109.425119
55	0.14529	3	230.2154643

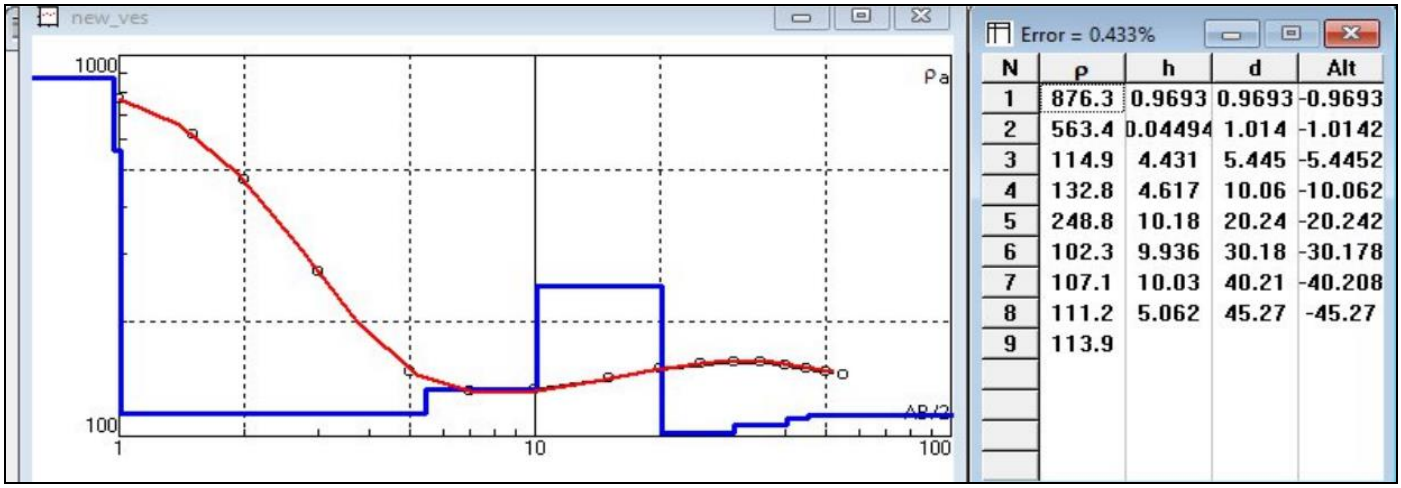

Fig 6 1D Electrical Resistivity Model for VES6

Table 7 Current Electrode Spacing, Potential Electrode Spacing, Measured Resistance, and Calculated Apparent Resistivity(Ωm) for VES7

AB/2 (m)	Resistance (Ω)	Mn/2 (m)	Apparent Resistivity(Ωm)
1	57.347	0.5	180.2334286
1.5	13.54	0.5	95.74714286
2	3.8546	0.5	48.45782857
3	2.3246	0.5	65.75297143
5	1.3214	0.5	103.8242857
7	1.0551	0.5	162.4854
7	4.6947	3	120.4973
10	2.6493	3	138.7728571
15	1.6993	3	200.2746429
20	1.1398	3	238.8152381
25	0.32193	3	105.39375
30	0.16851	3	79.44042857
35	0.05324	3	34.16233333
40	0.070516	3	59.09912381
45	0.021029	3	22.30576071
50	0.01977	3	25.88928571
55	0.11643	3	184.4861071

ISSN No: -2456-2165 https://doi.org/10.38124/ijisrt/26mar1483

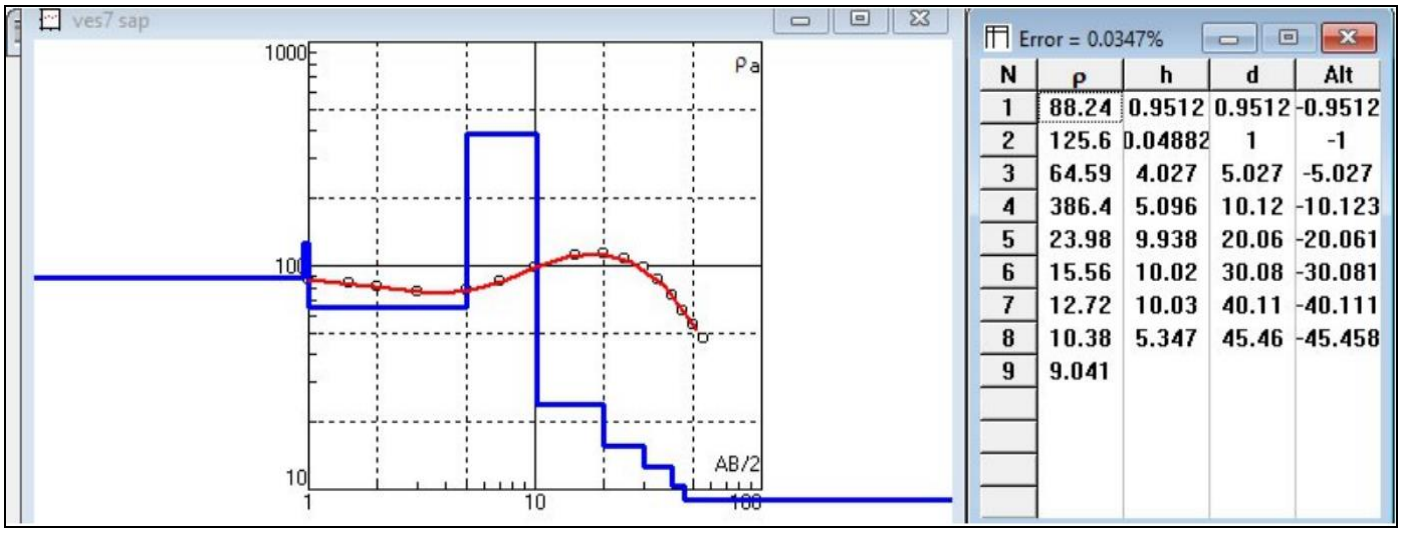

Fig 7 1D Electrical Resistivity Model for VES7

Table 8 Current Electrode Spacing, Potential Electrode Spacing, Measured Resistance, and Calculated Apparent Resistivity(Ωm) for VES8

AB/2 (m)	Resistance (Ω)	Mn/2 (m)	Apparent Resistivity(Ωm)
1	139.35	0.5	437.9571429
1.5	41.677	0.5	294.7159286
2	10.767	0.5	135.3565714
3	2.4054	0.5	68.03845714
5	0.65429	0.5	51.4085
7	0.14715	0.5	22.6611
7	3.7472	3	96.17813333
10	0.87185	3	45.66833333
15	0.22938	3	27.03407143
20	0.20175	3	42.27142857
25	0.10318	3	33.77916667
30	0.090538	3	42.6822
35	0.08812	3	56.54366667
40	0.069836	3	58.52921905
45	0.065404	3	69.37495714
50	0.077668	3	101.7080952
55	0.038557	3	61.09448452

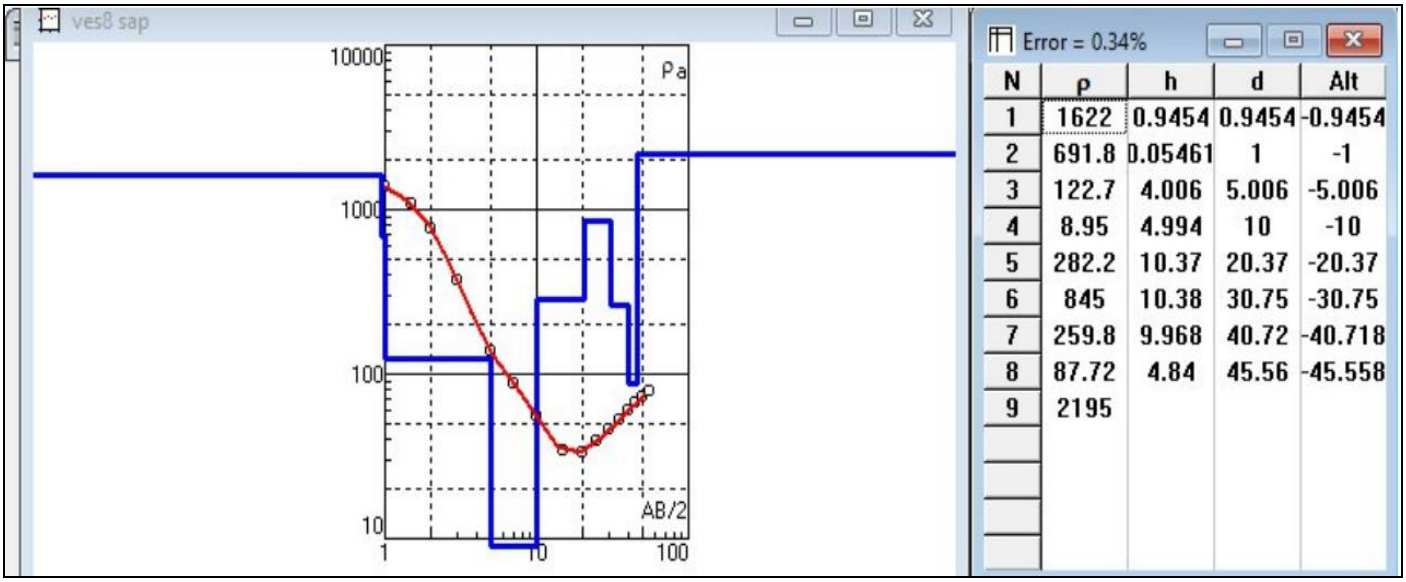

Fig 8 1D Electrical Resistivity Model for VES8

ISSN No: -2456-2165 https://doi.org/10.38124/ijisrt/26mar1483

➢ *2D Electrical Resistivity Models*

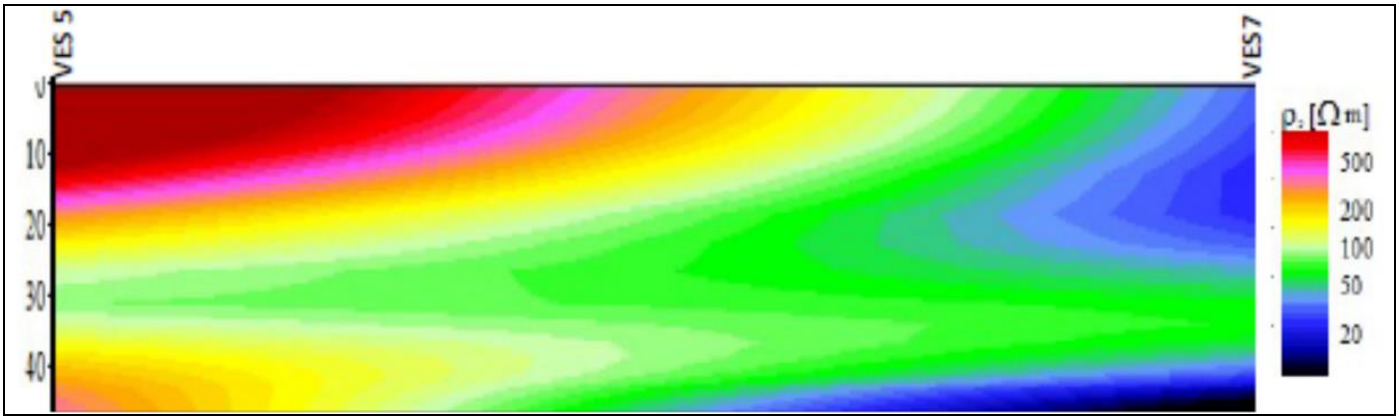

Fig 9 2D Electrical Resistivity Model for VES 5 and VES 7

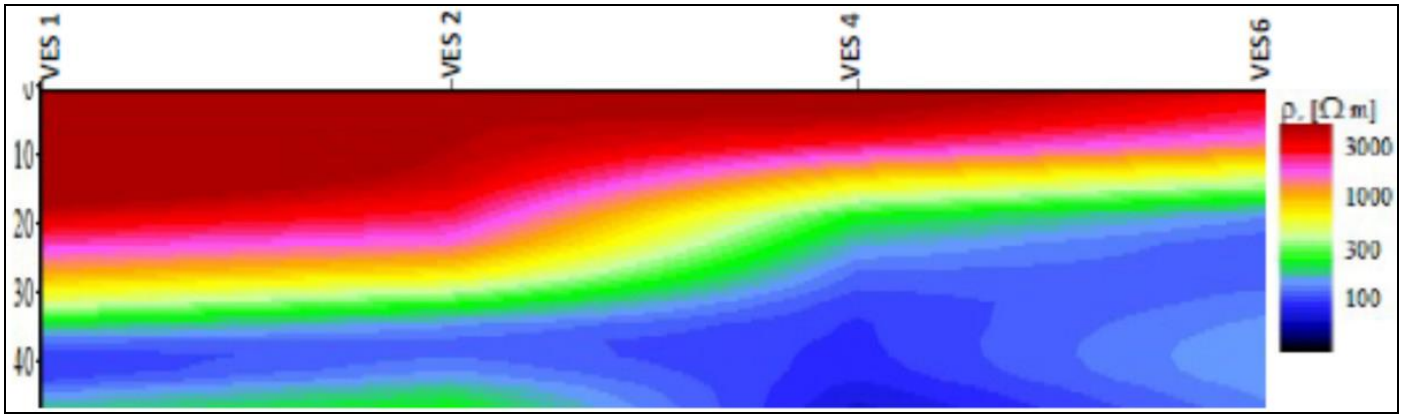

Fig 10 2D Electrical Resistivity Model for VES 1, VES 2, VES 4 and VES 6

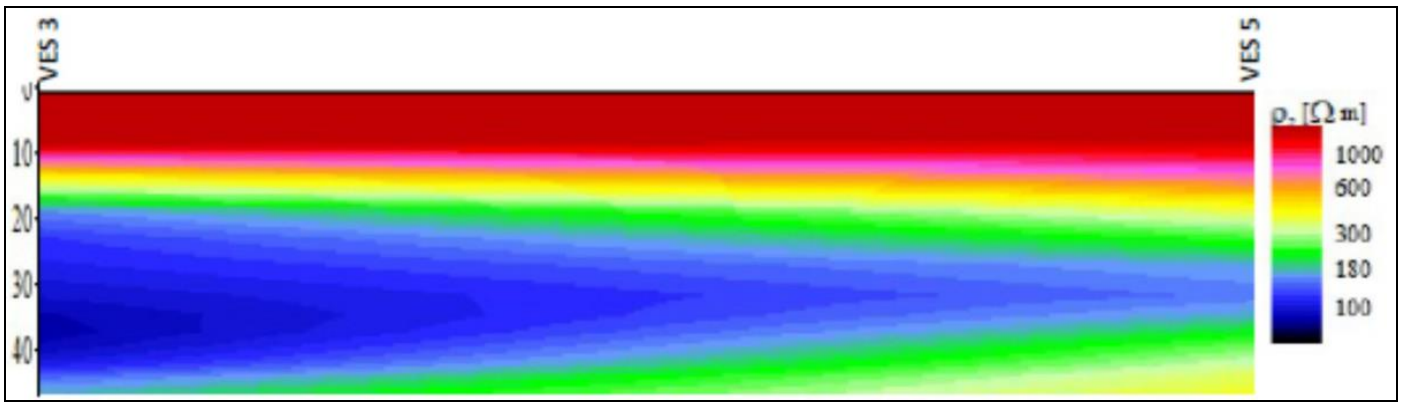

Fig 11 2D Electrical Resistivity Model for VES 3 and VES 5

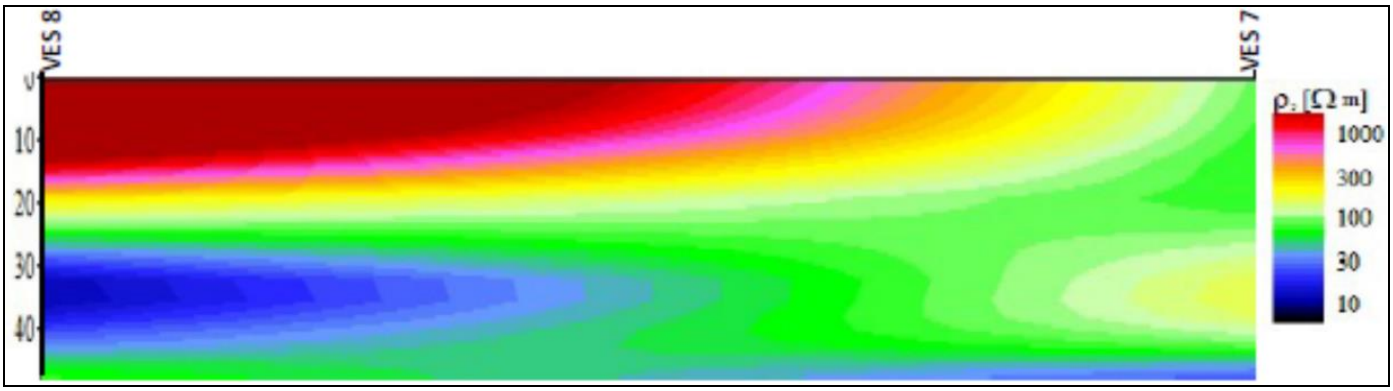

Fig 12 2D Electrical Resistivity Model for VES 8 and VES 7

ISSN No: -2456-2165 https://doi.org/10.38124/ijisrt/26mar1483

➢ *3D Electrical Resistivity Model*

Table 9 Resistivity Values at Different Depth

Depth (m)	VES1 Resistivity (Ωm)	VES2 Resistivity (Ωm)	VES3 Resistivity (Ωm)	VES4 Resistivity (Ωm)	VES5 Resistivity (Ωm)	VES6 Resistivity (Ωm)	VES7 Resistivity (Ωm)	VES8 Resistivity (Ωm)
0	1598	850	788	1227	535.5	876.3	88.24	1622
5	561	599	104	169.8	180.9	114.9	64.59	122.7
30	3314	165	684	7386	342.1	102.3	150.56	845
45	5811	613	928	333.4	153.8	111.2	10.38	87.72

Table 10 Coordinate of VES Point in Degrees Minutes and Seconds

VES Point	Degree N	Minutes N	Seconds N	Degree E	Minutes E	Seconds E
VES1	5	53	52.25	5	35	2.76
VES2	5	53	52.3	5	35	3.41
VES3	5	53	52.01	5	35	4.14
VES4	5	53	52.93	5	35	6.3
VES5	5	53	54.49	5	35	4.9
VES6	5	53	53.06	5	35	6.99
VES7	5	53	51.07	5	35	5.99
VES8	5	53	50.88	5	35	5.03

Table 11 Coordinate Points and Resistivity Values at 0m Depth

Latitude (Degree)	Longitude (Degree)	Resistivity (Ωm)
5.5841	5.897847222	1598
5.584280556	5.897861111	850
5.584483333	5.897780556	788
5.585083333	5.898036111	1227
5.584694444	5.898469444	535.5
5.585275	5.898072222	876.3
5.584997222	5.897519444	88.24
5.584730556	5.897466667	1622

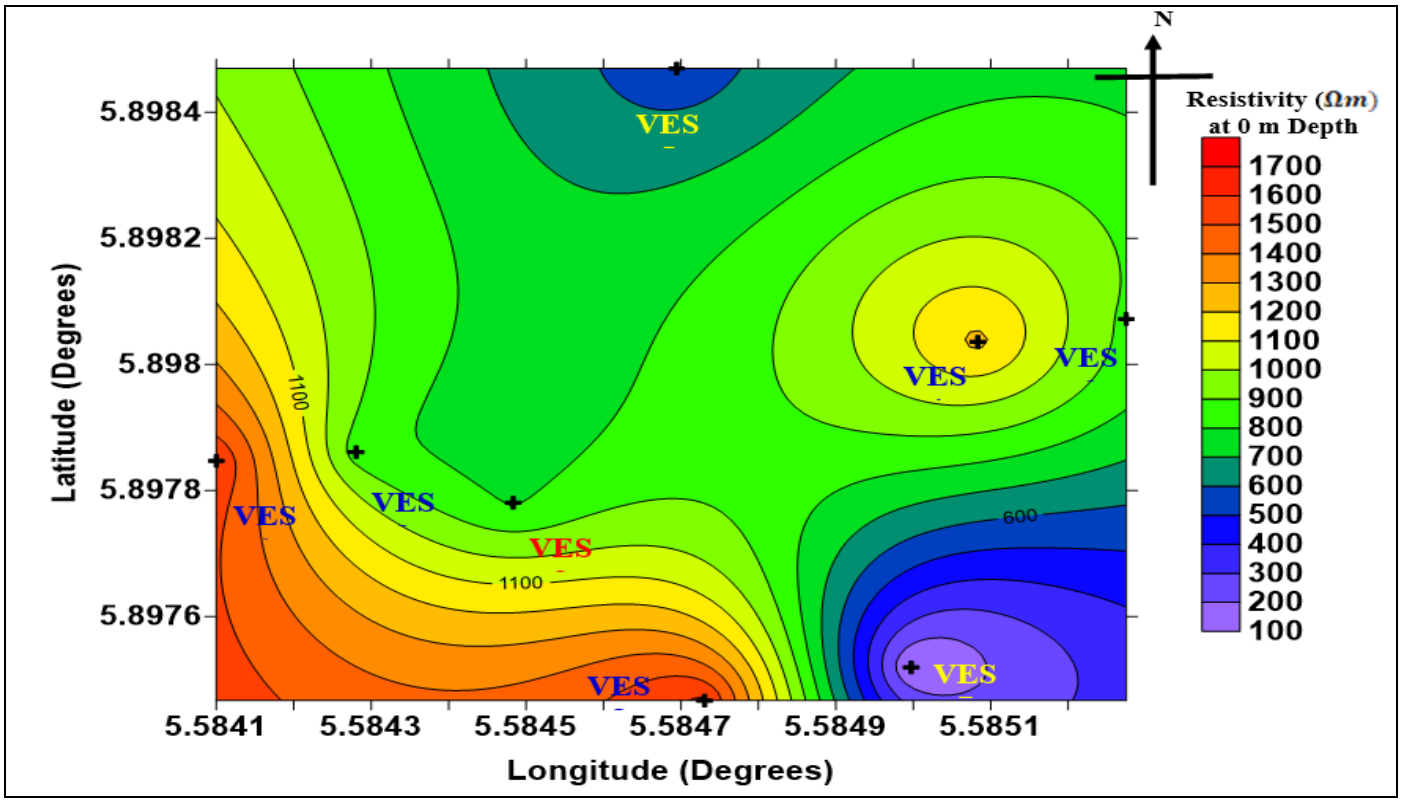

Fig 13 Contour Map Surface Distribution of Resistivity at a Depth of 0m

ISSN No: -2456-2165 https://doi.org/10.38124/ijisrt/26mar1483

Table 12 Coordinate Points and Resistivity Values at 5m Depth

Latitude (Degree)	Longitude (Degree)	Resistivity (Ωm)
5.5841	5.897847222	561
5.584280556	5.897861111	599
5.584483333	5.897780556	104
5.585083333	5.898036111	169.8
5.584694444	5.898469444	180.9
5.585275	5.898072222	114.9
5.584997222	5.897519444	64.59
5.584730556	5.897466667	122.7

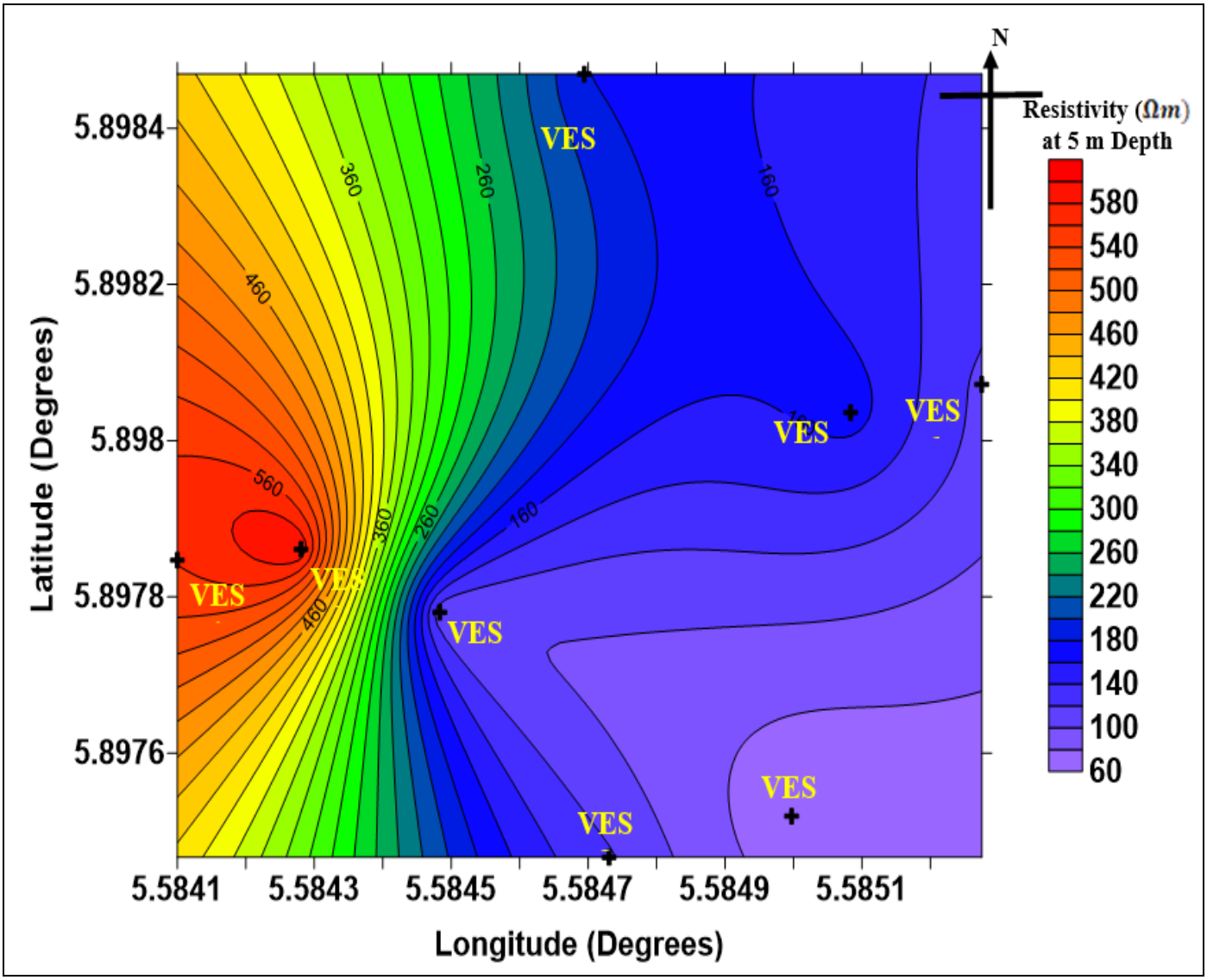

Fig 14 Contoured Surface Distribution of Resistivity at a Depth of 5m

Table 13 Coordinate Points and Resistivity Values at 30 m Depth

Latitude (Degree)	Longitude (Degree)	Resistivity (Ωm)
5.5841	5.897847222	3314
5.584280556	5.897861111	165
5.584483333	5.897780556	684
5.585083333	5.898036111	7386
5.584694444	5.898469444	342.1
5.585275	5.898072222	102.3
5.584997222	5.897519444	150.56
5.584730556	5.897466667	845

ISSN No: -2456-2165 https://doi.org/10.38124/ijisrt/26mar1483

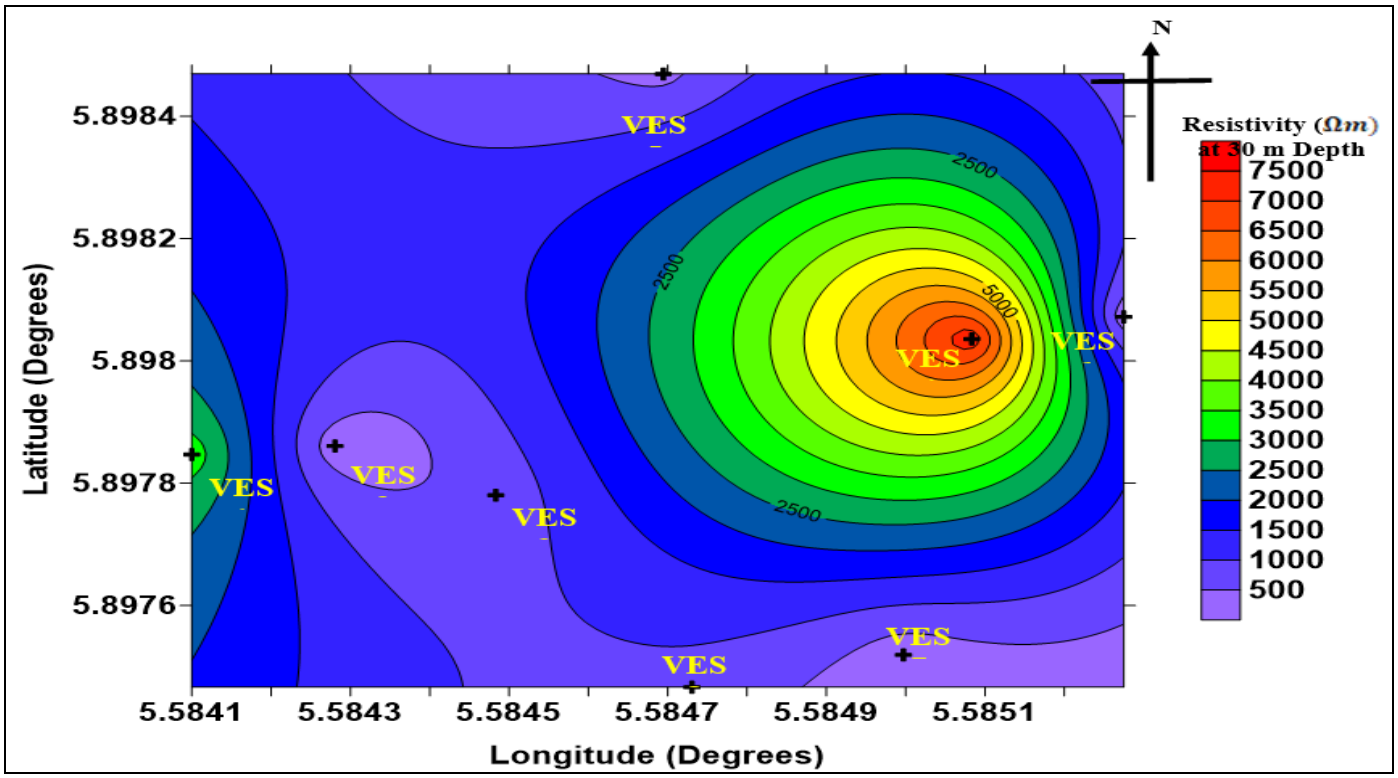

Fig 15 Contoured Map Surface Distribution of Resistivity at a Depth of 30m

Table 14 Coordinate Points and Resistivity Values at 45 m Depth

Latitude (Degree)	Longitude (Degree)	Resistivity (Ωm)
5.5841	5.897847222	5811
5.584280556	5.897861111	613
5.584483333	5.897780556	928
5.585083333	5.898036111	333.4
5.584694444	5.898469444	153.8
5.585275	5.898072222	111.2
5.584997222	5.897519444	10.38
5.584730556	5.897466667	87.72

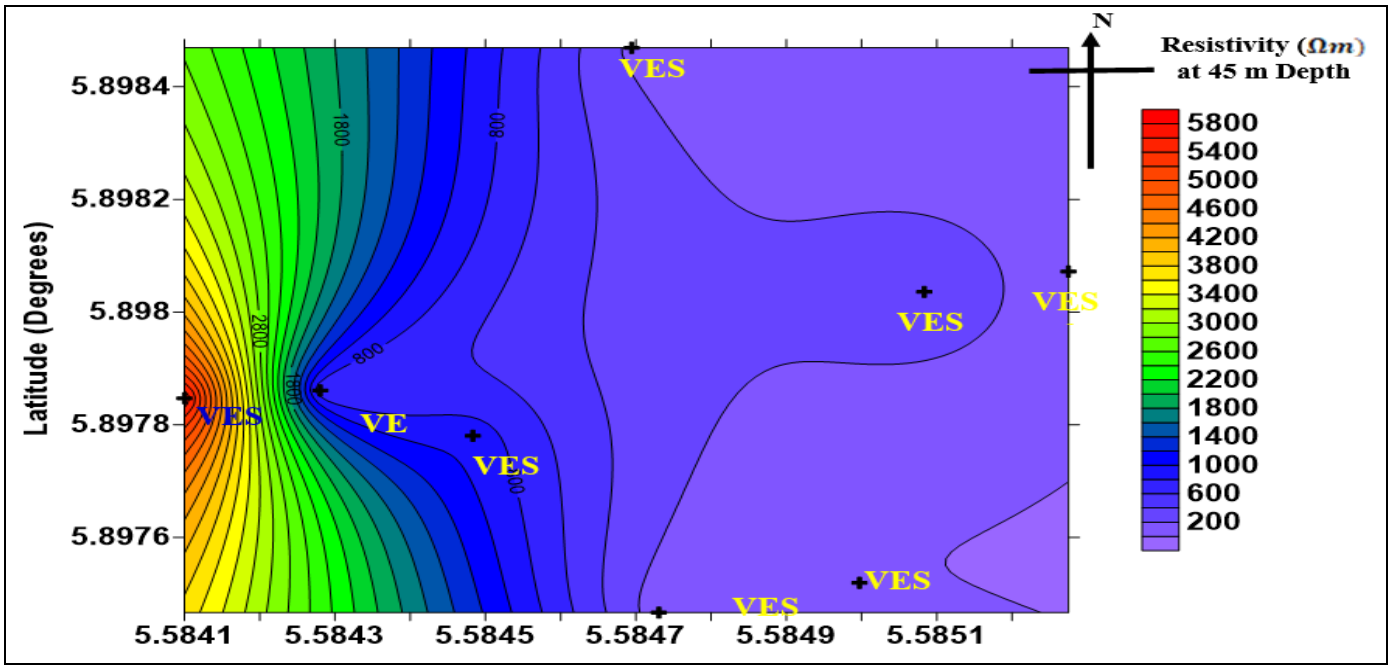

Fig 16 Contoured Surface Distribution of Resistivity at a Depth of 45m

ISSN No: -2456-2165 https://doi.org/10.38124/ijisrt/26mar1483

➢ *Quantitative Corrosion-Risk Evaluation*

To translate resistivity results into engineering-relevant corrosion assessments, subsurface materials were classified using established resistivity threshold as shown below:

- > 200 Ωm: Low corrosion risk
- 100–200 Ωm: Mild to moderate corrosion risk
- 50–100 Ωm: High corrosion risk
- < 50 Ωm: Very high corrosion risk

Applying this classification indicates that the near-surface zone (0–5m depth) constitutes a low-risk environment for buried metallic infrastructure. Conversely, deeper clay-dominated layers fall within high to very high corrosion-risk categories and are unsuitable for direct pipeline installation without mitigation.

IV. DISCUSSION AND CONCLUSION

The electrical resistivity results obtained from the 1D, 2D, 3D, and depth-slice models provide critical insight into the subsurface conditions controlling corrosion risk for buried pipelines and underground facilities within the study area. The dominance of high resistivity values in the near-surface zone reflects favourable geotechnical and electrochemical conditions for pipeline installation, while deeper low-resistivity horizons highlight potential corrosion challenges associated with clay-rich strata.

➢ *Interpretation of Near-Surface High-Resistivity Zone*

The near-surface resistivity values, predominantly exceeding 1700 Ωm down to an average depth of 5 m, are characteristic of sandy lithologies with low clay content and limited pore-water connectivity. Such materials exhibit poor ionic conductivity and therefore restrict the flow of galvanic and stray electrical currents. Numerous studies have established that soils with resistivity values greater than 200 Ωm are generally classified as low-corrosivity environments for metallic pipelines [4], [11].

In deltaic environments such as the Niger Delta, near-surface sands of the Benin Formation are typically well-drained and weakly cemented, resulting in high electrical resistivity [17], [6]. The resistivity distribution observed in this study is therefore consistent with the known geological framework of the region and supports the interpretation of a laterally continuous, corrosion-resistant layer suitable for shallow pipeline burial.

➢ *Low-Resistivity Horizons and Corrosion Implications*

Below the 5 m depth, resistivity values decrease sharply to ranges between 50 Ωm and 120 Ωm, particularly within the 20–30 m depth interval. These low-resistivity values are indicative of clay-rich horizons with high moisture retention and elevated ionic concentration. Clay minerals possess large surface areas and cation-exchange capacities that enhance electrical conductivity, thereby promoting electrochemical corrosion processes [18], [3]. According to standard corrosion-risk classifications, soils with resistivity below 100 Ωm are associated with high to very high corrosion risk [16], [11]. The presence of such horizons at depth implies that pipelines installed within or in direct contact with these materials would be vulnerable to accelerated corrosion unless appropriate mitigation measures, such as cathodic protection or resistivity modification through backfill replacement, are implemented.

➢ *Lateral Variability and Engineering Significance*

The 2D resistivity sections and depth-slice contour maps reveal that although the near-surface high-resistivity layer is laterally extensive, localized low-resistivity anomalies occur sporadically. These anomalies likely represent isolated clay lenses or zones of increased moisture content resulting from heterogeneity in depositional processes typical of deltaic systems [13], [10].

From an engineering perspective, such localized conductive zones are critical because they can act as preferential pathways for current leakage and initiate differential corrosion cells along pipeline segments. Even when average site resistivity values indicate low corrosion risk, these heterogeneities can significantly influence localized corrosion behavior [15]. This underscores the importance of spatially resolved resistivity imaging rather than reliance on point-based or averaged measurements.

- *Implications for Pipeline Burial Depth and Design:*

The integration of resistivity results with quantitative corrosion thresholds provides a defensible basis for defining safe pipeline burial depths. The findings indicate that burial within the upper 5 m of the subsurface offers a low-corrosion-risk environment, consistent with recommendations from corrosion engineering standards that prioritize installation in electrically resistive soils where feasible [2].

However, where engineering constraints necessitate deeper burial or where pipelines intersect low-resistivity zones, additional corrosion-control strategies become essential. These include the use of high-resistivity backfill materials, improved coating systems, and appropriately designed cathodic protection systems. Such integrated design approaches are widely recognized as best practice in pipeline integrity management [11].

- *Methodological Reliability:*

The consistency between the 1D VES interpretations, 2D resistivity sections, 3D models, and depth-slice maps enhances confidence in the reliability of the resistivity-derived corrosion assessment. Electrical resistivity methods have been shown to be particularly effective for identifying lithological contrasts and moisture-related conductivity variations that directly influence corrosion processes [5]. [14]. The multi-scale modelling approach adopted in this study therefore represents a robust framework for site-specific corrosion-risk evaluation.

REFERENCES

[1]. Akujieze, C.N., “Effects of Anthropogenic Activities (Sand Quarrying and Waste Disposal) on Urban

ISSN No: -2456-2165 https://doi.org/10.38124/ijisrt/26mar1483

Groundwater System and Aquifer Vulnerability Assessment in Benin City, Edo State, Nigeria", PhD Thesis, University of Benin, Benin City, Nigeria, 2004.

[2]. AMPP (Association for Materials Protection and Performance), "Standard Practice for Control of External Corrosion on Underground or Submerged Metallic Piping Systems", AMPP Standard SP0169-2020.

[3]. ASTM G187-12, "Standard Test Method for Measurement of Soil Resistivity Using the Two-Electrode Soil Box Method", ASTM International, West Conshohocken, PA, 2012.

[4]. Baeckmann, W.V., Schwenk, W. and Prinz, W., Handbook of Cathodic Corrosion Protection. 3rd edition. Gulf Professional Publishing, 1997.

[5]. Loke, M.H., Chambers, J.E., Rucker, D.F., Kuras, O. and Wilkinson, P.B., "Recent developments in the direct-current geoelectrical imaging method", Journal of Applied Geophysics, 95, pp.135-156, 2013.

[6]. Nwajide, C.S., "A guide to geological field trips to Anambra and related basins in Southeastern Nigeria", Great AP Express Publishers Ltd, 2005.

[7]. Obrike, S.E., "Evaluation of Imo clay-shale deposit (Paleocene) from Okada, Edo State, Southwestern Nigeria, as drilling mud clay", Journal of Applied Technology of Environmental Sanitation, 1(4), pp.311-316, 2012.

[8]. Obrike, S.E., Osadebe, C.C. and Onyeobi, T.U.S., "Mineralogical, geochemical, physical and industrial characteristics of shale from Okada area, southwestern Nigeria", Journal of Mining and Geology, 43(2), pp.109-116, 2007.

[9]. Okoye, I.P. and Obi, C., "Synthesis and Characterization of Al-Pillared Bentonite Clay Minerals", Research Journal of Applied Sciences, 6, pp.447-450, 2011.

[10]. Onyekuru, S.O., Iwuoha, P.O., Iwuagwu, C.J., Nwozor, K.K. and Opara, K.D., "Mineralogical and geochemical properties of Clay deposits in parts of Southeastern Nigeria", International Journal of Physical Sciences, 13(14), pp.217-229, 2018.

[11]. Peabody, A.W. and Bianchetti, R.L., "Peabody's Control of Pipeline Corrosion", 3rd edition. NACE International, 2017.

[12]. Petters, S.W. and Ekweozor, C.M., "Origin of Cretaceous black shales in the Benue Trough, Nigeria", Journal of Palaeogeography Palaeoclimatology Palaeoecology, 40, pp.311-319, 1981.

[13]. Reyment, R.A., "Aspects of the Geology of Nigeria", Ibadan University Press, Ibadan, 1965.

[14]. Reynolds, J.M., "An Introduction to Applied and Environmental Geophysics", 2nd edition. Wiley-Blackwell, 2011.

[15]. Roberge, P.R., "Corrosion Engineering: Principles and Practice", McGraw-Hill, 2008.

[16]. Romanoff, M., "Underground Corrosion. National Bureau of Standards Circular 579", U.S. Government Printing Office, Washington, D.C., 1957.

[17]. Short, K.C. and Stauble, A.J., "Outline of the Geology of Onitsha, Owerri and Benue Provinces", Geological Survey of Nigeria, Bulletin No. 21, 1967.

[18]. Uhlig, H.H. and Revie, R.W., "Corrosion and Corrosion Control", An Introduction to Corrosion Science and Engineering. 4th edition. John Wiley & Sons, 2008.